Molecular Cell
Short Article

Structure of a Multipartite Protein-Protein Interaction Domain in Splicing Factor Prp8 and Its Link to *Retinitis Pigmentosa*

Vladimir Pena,[1] Sunbin Liu,[2] Janusz M. Bujnicki,[3,4] Reinhard Lührmann,[2] and Markus C. Wahl[1,*]
[1] AG Röntgenkristallographie
[2] Abteilung Zelluläre Biochemie
Max-Planck-Institut für Biophysikalische Chemie, Am Fassberg 11, D-37077 Göttingen, Germany
[3] Laboratory of Bioinformatics and Protein Engineering, International Institute of Molecular and Cell Biology, Trojdena 4, 02-109 Warsaw, Poland
[4] Institute of Molecular Biology and Biotechnology, Adam Mickiewicz University, Umultowska 89, 61-614 Poznan, Poland
*Correspondence: mwahl@gwdg.de
DOI 10.1016/j.molcel.2007.01.023

SUMMARY

Protein Prp8 interacts with several other spliceosomal proteins, snRNAs, and the pre-mRNA and thereby organizes the active site(s) of the spliceosome. The DEAD-box protein Brr2 and the GTPase Snu114 bind to the Prp8 C terminus, a region where mutations in human Prp8 are linked to the RP13 form of *Retinitis pigmentosa*. We show crystallographically that the C-terminal domain of yeast Prp8p exhibits a Jab1/MPN-like core known from deubiquitinating enzymes. Insertions and terminal appendices are grafted onto this core, covering a putative isopeptidase center whose metal binding site is additionally impaired. Targeted yeast-two-hybrid analyses show that the RP13-linked region in the C-terminal appendix of human Prp8 is essential for binding of human Brr2 and Snu114, and that RP13 point mutations in this fragment weaken these interactions. We conclude that the expanded Prp8 Jab1/MPN domain represents a pseudoenzyme converted into a protein-protein interaction platform and that dysfunction of this platform underlies *Retinitis pigmentosa*.

INTRODUCTION

Most eukaryotic pre-mRNAs contain noncoding regions that have to be removed before translation. A multisubunit RNA-protein enzyme, the spliceosome, is responsible for catalyzing the two transesterification reactions of this pre-mRNA splicing (Will and Lührmann, 2006). With the help of numerous protein factors, the spliceosome is assembled on the pre-mRNA substrate from uridine-rich small nuclear ribonucleoprotein particles (U snRNPs), each of which is composed of a unique snRNA, seven Sm or Lsm proteins, and a variable number of particle-specific proteins (Will and Lührmann, 2006).

The catalytic activity of the spliceosome is presumably embodied in a network formed by snRNAs and the pre-mRNA (Valadkhan and Manley, 2001). However, none of the spliceosomal building blocks provides a preformed active center, and proteins are required to guide its formation, support its integrity, and mediate its disassembly (Staley and Guthrie, 1998). In particular, the proteins Brr2, Snu114, and Prp8 from the U5 snRNP are central to these processes. The ATPase/helicase activity of the DEAD-box protein Brr2 promotes both the catalytic activation (Kim and Rossi, 1999; Laggerbauer et al., 1998; Raghunathan and Guthrie, 1998) and disassembly (Small et al., 2006) of the spliceosomal RNA network. It is controlled by the GTPase Snu114 (Small et al., 2006). Prp8 is the largest (~280 kDa in yeast) and one of the most highly conserved spliceosomal proteins, and it is envisioned as an assembly platform in the spliceosome (Grainger and Beggs, 2005). It contacts all functionally important regions of the pre-mRNA, i.e., the 5′ splice site, the 3′ splice site, and the branch-point sequence, as well as U5 and U6 snRNAs, which are present in the catalytically activated spliceosome (Grainger and Beggs [2005] and references therein). Genetic interactions among Prp8p, Brr2p, and Snu114p in yeast (Brenner and Guthrie, 2005; Kuhn et al., 2002; van Nues and Beggs, 2001) and strong physical interactions between human (h) Prp8, hBrr2, and hSnu114 (Achsel et al., 1998) suggest that Prp8 controls the Brr2/Snu114 machinery. Yeast-two-hybrid (Y2H) analyses involving yeast (van Nues and Beggs, 2001) and human proteins (Liu et al., 2006) and a transposon-based dissection of yeast Prp8p (Boon et al., 2006) showed that Prp8 employs predominantly its N- and C-terminal regions to engage in protein-protein interactions. Conversely, RNA interactions have been mapped primarily to the central part of Prp8 (Reyes et al., 1999; Turner et al., 2006).

Apart from its fundamental functions in the spliceosome, Prp8 is interesting for medical reasons. *Retinitis*

Table 1. Crystallographic Data and Refinement

Data Collection				
Dataset	Native	SeMet Peak	SeMet Infl. Point	SeMet HE[a] Remote
Wavelength (Å)	1.05	0.97890	0.97920	0.95000
Space group	$P4_22_12$	$P4_22_12$		
Unit cell (Å)	a = b = 78.5 c = 122.8	a = b = 78.4 c = 122.8		
Resolution (Å)	30.0–2.0 (2.05–2.00)[b]	30.0–2.39 (2.49–2.39)	30.0–2.39 (2.49–2.39)	30.0–2.32 (2.42–2.32)
Reflections				
Unique[c]	26,084 (2003)	28,681 (3299)	28,845 (3337)	31,580 (3651)
Redundancy	4.8	9.5	6.9	7.0
Completeness (%)	97.8 (96.0)	98.4 (94.8)	99.0 (95.9)	99.0 (95.8)
$I/\sigma(I)$	16.1 (2.1)	18.6 (4.2)	16.1 (3.4)	15.2 (3.2)
R_{sym}[d]	11.2 (61.8)	9.5 (48.8)	9.6 (53.6)	9.8 (55.1)
Phasing				
Resolution (Å)		30.0–2.32		
Heavy atom sites		4		
Correl. coefficients[e]				
SHELXD CC/CC_{weak}		35.2/28.6		
SHELXE $CC_{overall}$		26.7		
CC_{free} left/right hand		64.3/38.3		
FOM[f]		0.60		
Refinement				
Resolution (Å)	30.0–2.0			
Reflections (#/%)	26,053/97.8			
Test set (%)	5			
R_{work}[g]	20.2			
R_{free}[g]	24.1			
ESU (Å)[h]	0.114			
Model				
Protein mol./res.	1/249			
Protein atoms	1995			
Water oxygens	312			
Mean B factors ($Å^2$)				
Wilson	27.8			
Protein	27.4			
Water	37.7			
Ramachandran plot				
Preferred	90.2			
Add. allowed	9.0			
Gen. allowed	0.4			
Disallowed	0.4			
Rmsd[f] geometry				
Bond lengths (Å)	0.010			
Bond angles (°)	1.19			

Table 1. (*continued*)

Rmsd B factors (Å^2)	
Main-chain bonds	0.72
Main-chain angles	1.25
Side-chain bonds	1.44
Side-chain angles	2.36
PDB entry	2OG4

[a] HE, high energy.
[b] Values for the highest resolution shell in parentheses.
[c] Numbers of unique reflections are given after averaging of Friedel pairs for the native data set and with Friedel pairs kept separate for SeMet data sets with anomalous signals.
[d] $R_{sym}(I) = (\Sigma_{hkl}\Sigma_i[|I_i(hkl) - \langle I(hkl)\rangle|] / \Sigma_{hkl}\Sigma_i[I_i(hkl)]$; $I_i(hkl)$, intensity of the ith measurement of hkl; $\langle I(hkl)\rangle$, average value of hkl for all i measurements.
[e] $CC = [\Sigma wE_oE_c\Sigma w - \Sigma wE_o\Sigma wE_c] / \{[\Sigma wE_o^2\Sigma_w - (\Sigma wE_o)^2][\Sigma wE_c^2\Sigma w - (\Sigma wE_c)^2]\}^{1/2}$; w, weight (see http://shelx.uni-ac.gwdg.de/SHELX/shelx_de.pdf for full definitions).
[f] FOM, figure of merit $= [|F(hkl)_{best}|] / |F(hkl)|$; $F(hkl)_{best} = \Sigma_\alpha[P(\alpha)F_{hkl}(\alpha)] / \Sigma_\alpha[P(\alpha)]$.
[g] $R_{work} = \Sigma_{hkl}[||F_{obs}| - k|F_{calc}||] / \Sigma_{hkl}[|F_{obs}|]$; $R_{free} = \Sigma_{hkl\subset T}[||F_{obs}| - k|F_{calc}||] / \Sigma_{hkl\subset T}[|F_{obs}|]$; hkl⊂T, test set.
[h] ESU, estimated overall coordinate error based on maximum likelihood.

pigmentosa is a frequently observed, progressive degeneration of the retina that leads to blindness. A severe form of the disease, RP13, has been linked to mutations in the very C-terminal portion of Prp8 (Grainger and Beggs [2005] and references therein). Apparently, the effects of these mutations on the function of this vital protein must be subtle, as so far the molecular basis for the disease has remained elusive.

Surprisingly few folded domains can be discerned based on the Prp8 sequence. An RNA recognition motif (RRM) and a Jab1/Mpr1/Pad1 N-terminal (Jab1/MPN) domain have been proposed in the center and at the C terminus, respectively (Grainger and Beggs, 2005; Maytal-Kivity et al., 2002). The Jab1/MPN motif is encountered in proteins with diverse functions in all domains of life (Maytal-Kivity et al., 2002). In the Rpn11 subunit of the proteasomal lid (Verma et al., 2002; Yao and Cohen, 2002) and the Csn5 subunit of the COP9 signalosome (Cope et al., 2002), it acts as a Zn^{2+}-dependent isopeptidase that cleaves bonds between lysine side chains of target proteins and the C termini of ubiquitin (Ub) or the Ub-like protein Nedd8, respectively. Although, in Prp8, some of the Zn^{2+} binding residues are not conserved and although mutational analyses have shown that Zn^{2+} binding by Prp8 is not vital in yeast (Bellare et al., 2006), it has been suggested that the protein may still support Zn^{2+} binding (Tran et al., 2003) and isopeptidase activity (Grainger and Beggs, 2005; Tran et al., 2003).

We were intrigued by a possible link between the putative Prp8 Jab1/MPN domain, the binding domain for Brr2 and Snu114, and the RP13 disease phenotype, all of which map to the C-terminal region of Prp8. To explore this potential link in more detail, we experimentally defined a folding unit at the C terminus of Prp8 encompassing the putative Jab1/MPN domain. We determined its crystal structure, which revealed that N- and C-terminal appendices and two insertions form a multiply connected layer on the surface of a Jab1/MPN-like core, in which the active site has been dismantled. RP13-related residues map to a short stretch in the C-terminal appendix. Exploiting this organization, we show by targeted Y2H analyses that the RP13-related region is essential for interaction with Brr2 and Snu114, and that RP13 point mutations differentially affect these interactions.

RESULTS AND DISCUSSION

Experimental Definition of a Folding Unit at the Prp8p C Terminus

Attempts to express C-terminal parts of hPrp8 resulted in insoluble aggregates. We, therefore, expressed residues 2112–2413 of *Saccharomyces cerevisiae* Prp8p (scPrp8p$^{2112–2413}$), which are 44% identical to hPrp8. scPrp8p$^{2112–2413}$ was purified to apparent homogeneity on SDS gels but did not crystallize in our hands, possibly owing to flexible regions. Treatment with chymotrypsin yielded a stable fragment starting with residue 2147 (Figure S1 in the Supplemental Data available with this article online). The 16 C-terminal amino acids of scPrp8p comprise an acidic tail, which may not form a stable structure. Therefore, we subcloned, expressed, and purified three smaller fragments: scPrp8p$^{2147–2413}$ (lacking the chymotrypsin-sensitive N-terminal part), scPrp8p$^{2112–2397}$ (lacking the acidic C-terminal part), and scPrp8p$^{2147–2397}$ (lacking both regions). Although all fragments were soluble and could be purified, only scPrp8p$^{2147–2397}$ reproducibly yielded well diffracting crystals (Table 1), suggesting that this fragment represents an ordered folding unit.

Crystal Structure Determination and Overall Fold

The crystal structure of scPrp8p$^{2147–2397}$ was solved by multiple anomalous dispersion (MAD) using a selenomethionine (SeMet)-substituted protein crystal and refined against 2.0 Å resolution data from a native crystal (Table 1

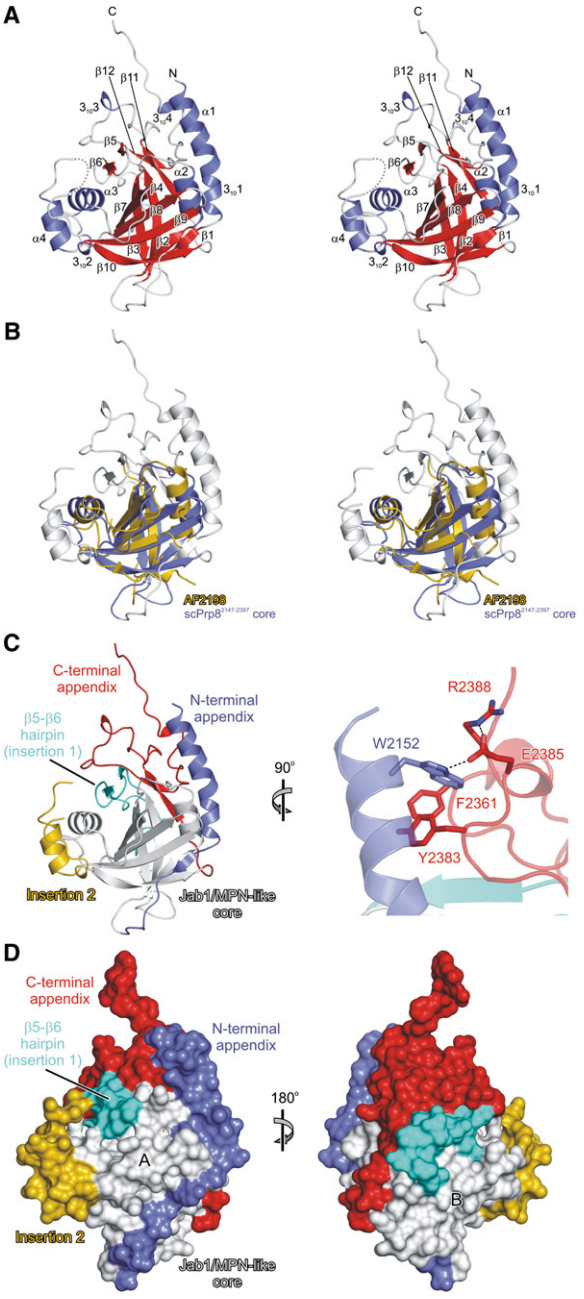

Figure 1. Structural Overview

(A) Stereo ribbon plot of scPrp8p$^{2147–2397}$. β strands, red; helices, blue; and coiled regions, gray. A short, disordered loop is shown as a dashed line.

(B) Stereo plot of an overlay of the Jab1/MPN domain of AF2198 (Ambroggio et al., 2004; Tran et al., 2003) on the present structure. scPrp8p$^{2147–2397}$ core, blue; periphery, gray; and AF2198, gold.

(C) Left, ribbon plot of scPrp8p$^{2147–2397}$ with structural elements color coded. Jab1/MPN-like core, gray; N-terminal extension, blue; β5-β6 hairpin (insertion 1), cyan; insertion 2, gold; and C-terminal extension, red. The coloring scheme is maintained in the subsequent figures. Right, close-up view of the interacting N- and C-terminal appendices. Interacting residues are shown as sticks and color coded by atom type (carbon, as the respective protein part; nitrogen, blue; and oxygen, red). Dashed lines indicate hydrogen bonds and salt bridges. The orientation relative to (C) is indicated.

(D) Surface views of scPrp8p$^{2147–2397}$.

and Figure S2). The final model exhibits good stereochemistry and encompasses residues 2148–2396. Residues 2321–2325 form a flexible loop that displays discontinuous density.

Consistent with our domain mapping, scPrp8p$^{2147–2397}$ exhibits a compact, oval-shaped fold containing 12 β strands (β1–β12), four α helices (α1–α4), and four 3_{10} helices (3_{10}1–3_{10}4; Figure 1A). The structure comprises a mixed, seven-stranded β barrel (strands β2–β4 and β7–β10), around which additional α- and β elements are arranged. Helix α1, which is contiguous with helix 3_{10}1, and helix α2 are parallel and form a lid on top of the barrel. The bottom of the barrel is uncovered. Helices α3 and α4 are perpendicular to each other and, together with a hairpin formed by strands β5 and β6, line one lateral side of the barrel. Two additional strands, β11 and β12, pair with the C-terminal half of strand β4 and affix the C-terminal portion of scPrp8p$^{2147–2397}$ to the barrel. R2388–S2396 at the very C terminus protrude from the compact portion (Figure 1A) and engage in crystal packing contacts with a neighboring molecule.

scPrp8p$^{2147–2397}$ Is Composed of a Jab1/MPN-like Core with Insertions and Appendices

The Jab1/MPN fold has so far been defined in two crystal structures of the product of *Archaeoglobolus fulgidus* open reading frame AF2198 (Ambroggio et al., 2004; Tran et al., 2003). We inspected the structure of scPrp8p$^{2147–2397}$ for a Jab1/MPN-like fold as expected from sequence analysis (Grainger and Beggs, 2005; Maytal-Kivity et al., 2002). The β barrel and helices α2 and α3 are constructed from three portions of the protein that are noncontiguous on the primary level (gray bars in Figure 2). These elements can be superimposed on the Jab1/MPN module of AF2198 (PDB IDs 1OI0 and 1R5X) with a root-mean-square deviation (rmsd) of 2.6 Å for 100 equivalent Cα atoms (Figure 1B). This structural similarity is remarkable considering the very low sequence identity between the two proteins (~14%; Figure S3). On average, the strands of scPrp8p$^{2147–2397}$ are longer and form a closed barrel, whereas the shorter strands in AF2198 are arranged into a highly bent β sheet. A portion corresponding to the β5-β6 hairpin of scPrp8p$^{2147–2397}$ (cyan in Figure 1C) could not be traced in AF2198. It is shorter by six residues in AF2198 and may adopt a different structure. Our structural analysis clearly demonstrates the presence of a Jab1/MPN-like core motif in scPrp8p$^{2147–2397}$.

Multiple sequence alignments show that scPrp8p$^{2147–2397}$ contains ~30 residues at its N terminus (blue bar in Figure 2) and ~45 residues at its C terminus (red bar) in addition to the Jab1/MPN domain. The N-terminal appendix encompasses the long helix composed

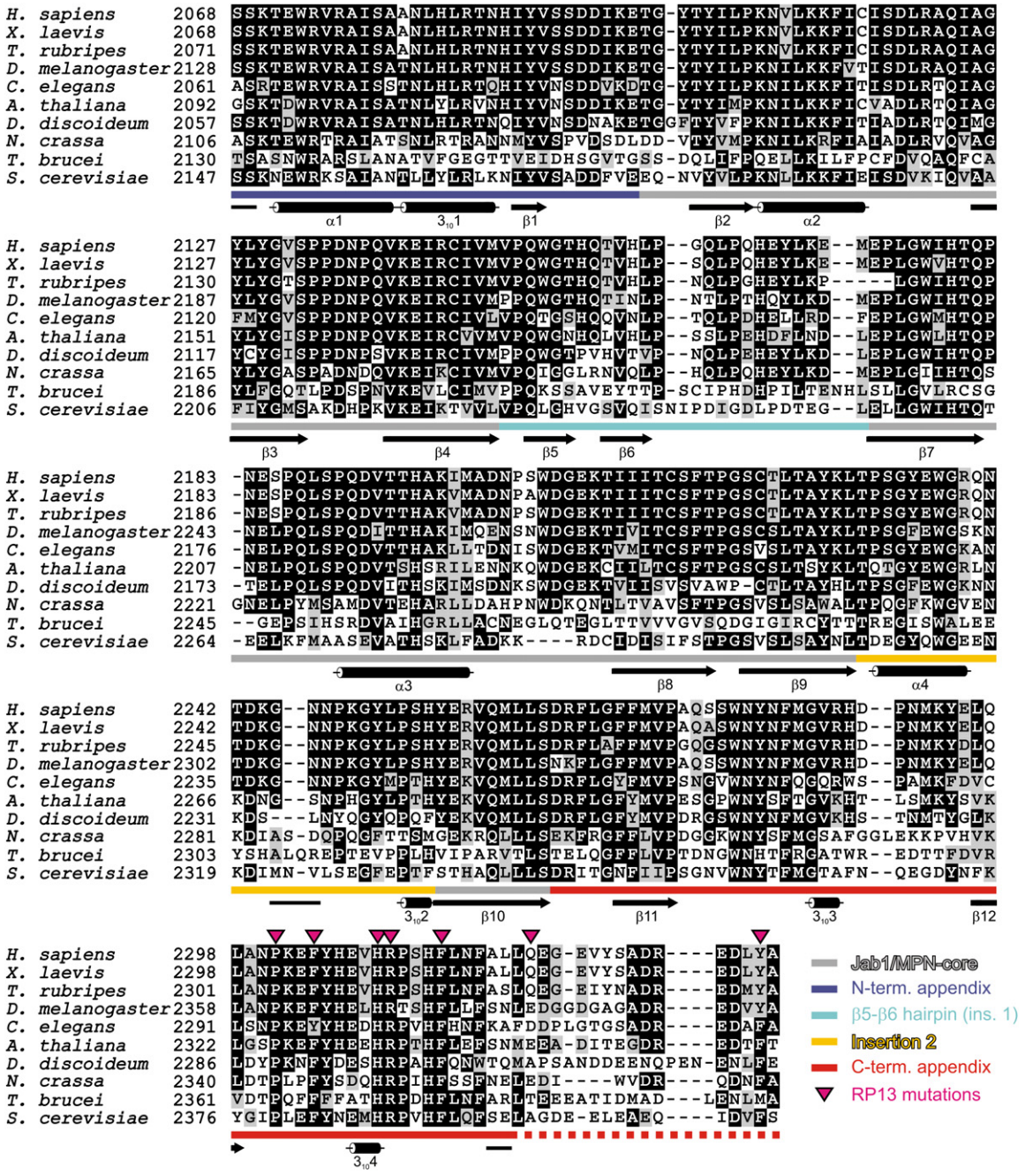

Figure 2. Multiple Sequence Alignment

Alignment of C-terminal regions from representative Prp8 orthologs. Darker background corresponds to higher conservation. Icons below indicate secondary structure elements from the scPrp8p$^{2147–2397}$ crystal structure. Colored bars below the alignment indicate structural portions of scPrp8p$^{2147–2397}$ (see legend). Magenta triangles indicate positions of RP13 point mutations.

of α1 and $3_{10}1$ (Figure 1C, blue). It continues with strand β1 that is wedged into the barrel by running alongside the C terminus of strand β9. A long loop links β1 to the first strand, β2, and encircles the last strand, β10, of the barrel. The C-terminal appendix follows strand β10 (Figure 1C, red). It forms a left-handed spiral that is stabilized by the antiparallel alignment of strands β11 and β12. Apart from the β5-β6 hairpin (Figure 1C, cyan), scPrp8p$^{2147–2397}$ harbors a second insertion of 25 residues, which encompasses helices α4 and $3_{10}2$ (Figure 1C, gold).

The N- and C-terminal appendices and the two insertions are tightly wrapped around the Jab1/MPN-like core (Figures 1C and 1D). The peripheral elements engage in multiple interactions with each other and thereby form

a frayed but contiguous layer that covers about 3100 Å^2 or 43% of the entire surface area of the core module. W2152 from helix α1 of the N-terminal appendix is deeply buried in a mixed hydrophilic and hydrophobic pocket formed by the C-terminal extension (Figure 1C, right). This interaction "seals" the appendices at positions close to their termini. About two-thirds of the interface between the peripheral elements and the core are hydrophobic, suggesting that the peripheral parts are stably and permanently grafted onto the core. An appendix wrapping around a protein core in a similar manner has been observed with cytochrome-c_{552} from *Thermus thermophilus*, where it was suggested to confer resistance against thermal denaturation (Than et al., 1997). Similarly, we expect that the insertions and appendices stabilize the scPrp8p Jab1/MPN-like core. Indeed, in contrast to the core alone (Bellare et al., 2006; Tran et al., 2003), the expanded motif could be easily expressed and purified (our results and Bellare et al. [2006]).

Our structure shows that residues, which are mutated in temperature-sensitive or lethal *prp8* alleles (Bellare et al., 2006; Schmidt et al., 1999; van Nues and Beggs, 2001) stabilize the fold of the Jab1/MPN-like core (alleles *spp42-1*, *prp8-28*, *prp8-601*, *prp8-602*, *prp8-603*, *prp8-605*, and *prp8-606*), the interaction between the core and the surface layer (*prp8-602*, *prp8-604*, *prp8-605*, *prp8-607*, and *prp8-608*), or interactions between and within surface layer elements (*spp42-1* and *prp8-608*; Figure S4). These observations suggest that the organization of scPrp8p$^{2147–2397}$ observed in the crystal is functionally important.

The Putative Active Site of scPrp8p$^{2147–2397}$ Is Deconstructed

Many of the Jab1/MPN family members contain a highly conserved $EX_nHXHX_7SX_2D$ fingerprint (X, any amino acid), termed the Jab1/MPN/Mov34 or Jab1/MPN domain metalloenzyme (JAMM) motif, which comprises a Zn^{2+} binding site. In AF2198, the two histidines (H67 and H69) and the aspartate (D80) directly coordinate a Zn^{2+} ion, whereas the glutamate (E22) and serine (S77) stabilize a catalytic, Zn^{2+}-bound water molecule (Ambroggio et al., 2004; Tran et al., 2003). In scPrp8p, the canonical JAMM motif is replaced by $Q^{2202}X_{57}H^{2260}XQ^{2262}X_9S^{2272}E^{2273}$.

Residues Q2202, H2260, Q2262, S2272, and E2273 of scPrp8p$^{2147–2397}$ cluster in the area corresponding to the Zn^{2+} binding site of AF2198 but adopt different rotamers from the AF2198 JAMM motif residues (Figure 3A). Instead of a metal ion, a chain of ordered water molecules is seen in scPrp8p$^{2147–2397}$ (Figure 3A) in agreement with the lack of an anomalous signal in the native diffraction data. Therefore, the amino acid replacements in the JAMM-like motif of scPrp8p$^{2147–2397}$ apparently impair Zn^{2+} binding. Our structure shows that no residues from other parts of the protein substitute for the missing functionalities of the motif. Because mutational analyses indicated that the JAMM motifs and Zn^{2+} binding in Rpn11 and Csn5 are essential for isopeptidase activity (Cope et al., 2002; Verma et al., 2002; Yao and Cohen, 2002), scPrp8p$^{2147–2397}$ can be considered a pseudoenzyme. In agreement with our observation that scPrp8p function does not rely on an intact Zn^{2+} binding site, the quadruple mutation Q2202A/H2260A/Q2262A/E2273A (*prp8-602*) of residues in the JAMM-like motif only leads to temperature sensitivity, i.e., a mild phenotype (Bellare et al., 2006).

In AF2198, the Zn^{2+} ion is bound at the bottom of a wide cleft and is exposed to the solvent (Figure 3B). In contrast, in scPrp8p$^{2147–2397}$, this site is covered by the β5-β6 hairpin (Figure 3B). The hairpin runs exactly along a hydrophobic groove in the core domain, which has previously been proposed to constitute a substrate binding site on enzymatically active Jab1/MPN domains (Ambroggio et al., 2004; Tran et al., 2003). It is possible that after the core had lost its enzymatic activity, β5-β6 was permanently inserted in the substrate binding pocket. The β5-β6 lid is wedged between the second insertion and the C-terminal appendix (Figures 1C and 1D) and thereby fastened in place. Thus, even if the active site were functional, the β5-β6 hairpin would effectively block access of a substrate peptide (Figure 3B).

Implications for Ubiquitin Binding by Prp8

A protein comprising residues 2143–2413 of scPrp8p was found to exhibit low affinity for Ub and thus possibly could interact with a ubiquitinated splice factor (Bellare et al., 2006). In light of other domains in the spliceosome that are related to Ub metabolism (Bellare et al. [2006] and references therein), these findings suggested a role for ubiquitination in pre-mRNA splicing. scPrp8p$^{2147–2397}$ structurally represents almost the entire Ub binding fragment of scPrp8p.

We reasoned that the Ub affinity of scPrp8p should be encoded in the Jab1/MPN-like core, because this unit is also contained in other Ub binding proteins, such as the Rpn11 and Csn5 isopeptidases (Cope et al., 2002; Verma et al., 2002; Yao and Cohen, 2002). If so, Ub binding should take place through a region of the Jab1/MPN-like core that is surface exposed in scPrp8p$^{2147–2397}$. Only two such surface patches can be discerned ("A" and "B" in Figure 1D). Both are neighboring the deconstructed metalloisopeptidase active site. Ub binding domains preferentially interact via a hydrophobic region with the conserved I44 of Ub (Bellare et al., 2006; Sloper-Mould et al., 2001). However, the A and B regions exhibit similarly mixed chemical compositions.

Two scPrp8p mutants have been shown to inhibit Ub affinity at 37°C, a quadruple mutant of JAMM-like residues (Q2202A/H2260A/Q2262A/E2273A; *prp8-602*), and the double mutant V2184A/L2185A (*prp8-603*) (Bellare et al., 2006). The JAMM-like motif is an unlikely binding site for Ub, because it is essentially not accessible. Thus, the effect of this mutation is most likely structural, affecting Ub affinity indirectly. Residues 2184–2185 are partially exposed at the surface and reside at one edge of exposed area B, supporting a role of area B in Ub binding. However,

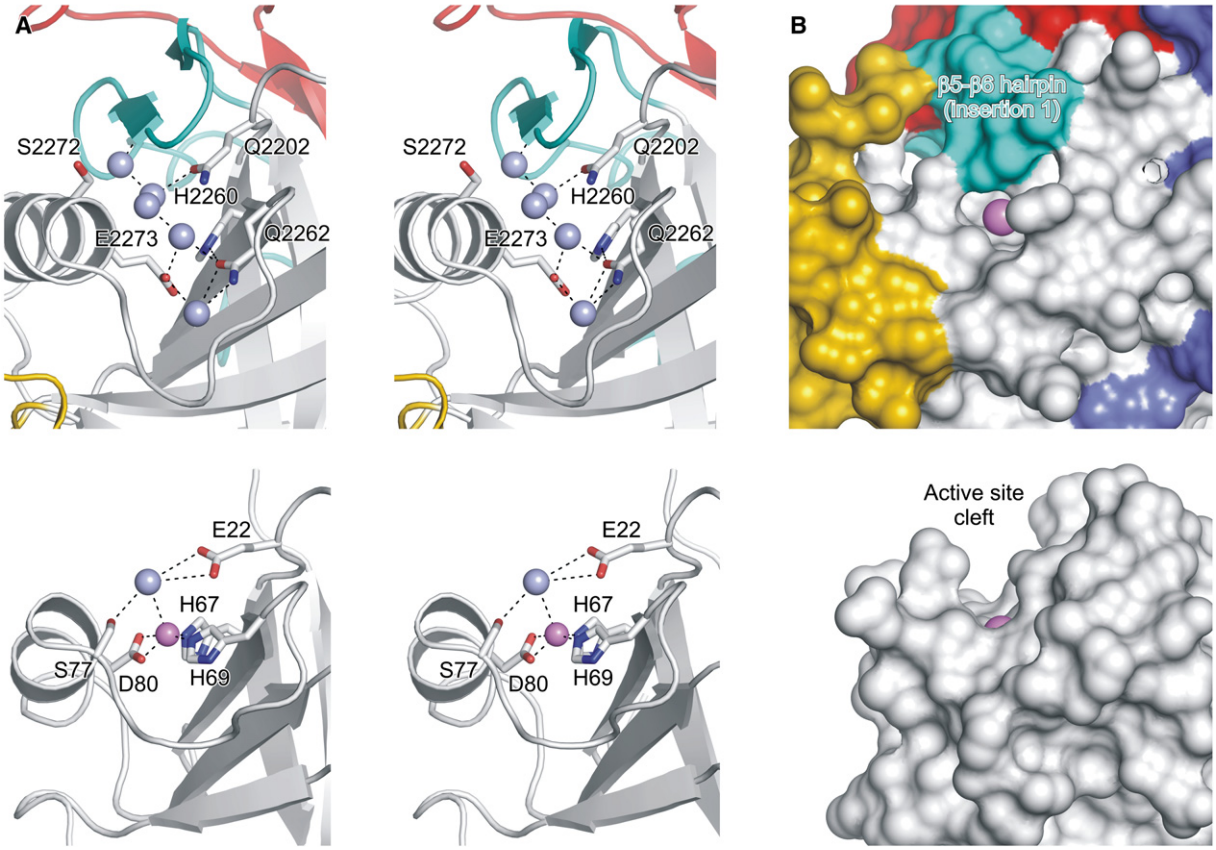

Figure 3. JAMM-like Motif in scPrp8p$^{2147–2397}$

(A) Top, stereo ribbon plot of the JAMM-like motif in scPrp8p$^{2147–2397}$ (orientation as in Figure 1A). Putative JAMM-like residues are shown as sticks and color coded by atom type. Light blue spheres, water molecules. Hydrogen bonds are indicated by dashed lines. Bottom, JAMM motif of AF2198 in an identical orientation. Violet sphere, Zn^{2+} ion. S2272 of scPrp8p$^{2147–2397}$ is the homologous residue closest in space to S77 of AF2198. An alanine is found at the scPrp8p$^{2147–2397}$ position equivalent to S77 (data not shown).

(B) Surface representation of the regions in A (scPrp8p$^{2147–2397}$, top; AF2198, bottom). The Zn^{2+} ion (violet sphere) was mapped on the structure of scPrp8p$^{2147–2397}$ by superimposition of AF2198.

ultimate clarification of the Ub binding site has to await future investigations.

RP13-Linked Mutations Cumulate in a Fragment Essential for Binding Brr2 and Snu114

All residues of hPrp8, which give rise to RP13 when mutated and which are represented in our structure, are absolutely conserved in yeast Prp8p (Figure 2), suggesting that these residues serve the same functions in the human and yeast proteins. Therefore, the effects of these RP13 mutations on the function of hPrp8 can be interpreted based on the scPrp8p$^{2147–2397}$ structure and vice versa.

The interaction of scBrr2p with scPrp8p was severely affected by a G2347D mutation (van Nues and Beggs, 2001). G2347 is located directly N-terminal of strand β11 in the C-terminal appendix, suggesting that our scPrp8p$^{2147–2397}$ fragment and in particular its C-terminal part could constitute a binding site for scBrr2p (Figure 4A). In agreement with this notion, the C-terminal ~100 residues of hPrp8 (hPrp8$^{2239–2335}$/scPrp8p$^{2315–2413}$) were recently shown to interact with hBrr2$^{1301–1816}$ (encompassing its second helicase domain), with hSnu114$^{603–972}$ (encompassing EF-2-homology domains IV and V), and with the N-terminal part of hPrp8 (hPrp8$^{1–387}$, equivalent to scPrp8p$^{1–461}$) (Liu et al., 2006). Our structure reveals that residues 2315–2413 of scPrp8p are wrapped around the Jab1/MPN core and encompass the entire C-terminal appendix (Figure 4A). It is obvious that the fragment hPrp8$^{2239–2335}$/scPrp8p$^{2315–2413}$ in isolation cannot maintain the structure it adopts in the framework of scPrp8p$^{2147–2397}$ (Figure 4A). These data suggest that an intact fold of the Jab1/MPN domain is not required for the interaction with hBrr2$^{1301–1816}$, hSnu114$^{603–972}$, and hPrp8$^{1–387}$. Rather, the C-terminal stretch of Prp8 could encompass linear interaction epitopes. The portion starting at R2310/R2388 separates from the body of the domain (Figure 4A) and is an attractive candidate epitope.

Conspicuously, RP13-linked point mutations lie in the C-terminal 35 residues of hPrp8 (Grainger and Beggs [2005] and references therein; Figure 4A), suggesting

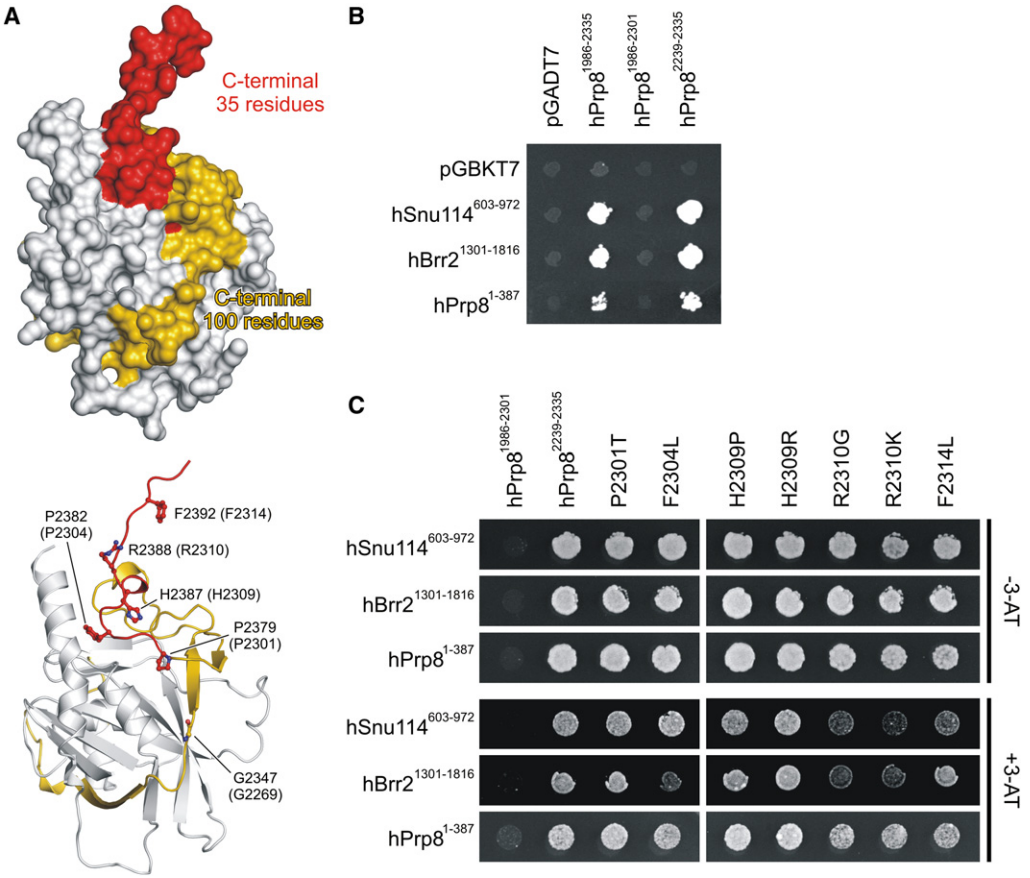

Figure 4. Protein-Protein Interactions at the C Terminus of scPrp8p$^{2147–2397}$

(A) Top, C-terminal 100 residues (gold and red) and the C-terminal 35 residues (red) of scPrp8p mapped on the surface of scPrp8p$^{2147–2397}$. The view is from the right compared to Figure 1A. Bottom, ribbon plot of scPrp8p$^{2147–2397}$ with the same color coding and orientation as above. Residue G2347, which upon mutation to an aspartate inhibits interaction with scBrr2p (van Nues and Beggs, 2001), and residues, which upon mutation elicit RP13, are indicated as sticks.

(B) Y2H analysis of hPrp8 fragments. Yeast strain AH109 was transformed with prey fusions of hPrp8 C-terminal fragments (residue ranges indicated) in combination with baits of hSnu114$^{603–972}$, hBrr2$^{1301–1816}$, and hPrp8$^{1–387}$. Interactions were observed at 30°C on SD/-Leu-Trp-His-Ade medium. Vectors pGADT7 or pGBKT7 were used as controls.

(C) Y2H examination of the RP13 point mutations based on hPrp8$^{2239–2335}$ as indicated above the panels. pGADT7-hPrp8$^{1986–2301}$ and pGADT7-hPrp8$^{2239–2335}$ (WT) are negative and positive controls, respectively. Protein-protein interactions were monitored on SD/-Leu-Trp-His-Ade (upper panel) and on SD/-Leu-Trp-His+3-AT (lower panel).

a link between the disease and aberrant interactions among hPrp8, hBrr2, and hSnu114. To test this possibility, we analyzed fragment hPrp8$^{1986–2301}$ (equivalent to scPrp8p$^{2058–2378}$), lacking these residues, in a targeted Y2H assay. In sharp contrast to hPrp8$^{1986–2335}$ or hPrp8$^{2239–2335}$, which contain the RP13-linked region, hPrp8$^{1986–2301}$ completely failed to interact with hSnu114$^{603–972}$, hBrr2$^{1301–1816}$, and hPrp8$^{1–387}$ (Figure 4B). We conclude that the C-terminal 35 residues of hPrp8 that contain all RP13-linked positions are essential for the interactions with hBrr2$^{1301–1816}$, hSnu114$^{603–972}$, and hPrp8$^{1–387}$.

The above results show that a short stretch in the C-terminal tail of Prp8 is essential for the interaction of at least three different proteins (Brr2, Snu114, and the N terminus of Prp8). The proteins could share one binding epitope, which they recognize concomitantly, or they could interact sequentially with the same or overlapping regions in Prp8. The latter picture would be in general agreement with the stepwise remodeling during spliceosome maturation, catalysis, and disassembly. Thus, the extended Prp8 Jab1/MPN-like domain could act as a relay station and thereby control the ATPase/helicase and GTPase activities of Brr2 and Snu114, respectively. Irrespective of the exact nature of the interactions, our results define the C-terminal extension of the Jab1/MPN-like domain of Prp8 orthologs as a major protein-protein interaction scaffold.

RP13-Linked Mutants Affect the Interaction of Prp8 with Brr2 and Snu114

We next asked whether the RP13-linked substitutions have any direct effect on the protein-protein interactions.

We introduced individually the seven RP13 point mutations P2301/2379T, F2304/2382L, H2309/2387P, H2309/2387R, R2310/2388G, R2310/2388K, and F2314/2392L (human/yeast numbering) into hPrp8$^{2239–2335}$ (equivalent to scPrp8p$^{2315–2413}$) and tested the interactions of the mutants with hSnu114$^{603–972}$, hBrr2$^{1301–1816}$, and hPrp8$^{1–387}$ (scPrp8p$^{1–461}$). No significant effects were observed under standard conditions (Figure 4C, upper). Under more stringent conditions (addition of 3-amino-1,2,4-triazole; 3-AT), mutating R2310/2388 to either G or K significantly reduced the interaction with hSnu114$^{603–972}$ and hBrr2$^{1301–1816}$, but not with hPrp8$^{1–387}$. Mutation F2314/2392L only diminished the interaction with hSnu114$^{603–972}$. F2304/2382L only affected the interaction with hBrr2$^{1301–1816}$. Mutants P2301/2379 and H2309/2387 again showed no effect. Consistent with a linear binding epitope, these results suggest that multiple closely spaced hPrp8 residues contribute to the interactions. The contributions of P2301/2379 and H2309/2387 may be too weak to detect in our experimental setup.

Implications for the Molecular Basis of RP13

These above results indicate that aberrant protein-protein interactions in the spliceosome constitute one molecular basis of RP13. The observation that individual RP13 mutations in hPrp8 weaken but do not abolish interactions with hBrr2 and hSnu114 could explain the tissue-specific phenotype of the disease; e.g., a retina-specific alternative splicing event may demand a strong interaction among the proteins investigated, whereas for the vast majority of splicing events, the affinities exhibited by the RP13-linked Prp8 point mutants are sufficient.

Not all RP13-linked positions in the C-terminal appendix of the Prp8 Jab1/MPN domain necessarily exert their effects through the protein-protein interactions tested herein. As seen in our structure, P2301/2379, F2304/2382, and H2309/2387 interact with other regions of the Jab1/MPN domain (Figure 4A), and mutation of these residues could therefore influence the structure of the module or its folding kinetics. Although misfolding of the Jab1/MPN domain per se does not corrupt interactions with hSnu114$^{603–972}$, hBrr2$^{1301–1816}$, or the N-terminal portion of hPrp8 (see above), aberrant folding or folding kinetics conceivably reduce the steady-state levels of functional Prp8 protein required for biogenesis of the U5 snRNP. As a consequence, steady-state levels of U5 snRNP or U4/U6-U5 tri-snRNP could be low and in turn be responsible for a tissue-specific splicing defect.

A New View on the Prp8 C Terminus: A Pseudoenzyme Converted into an Adaptor Module

Jab1/MPN domains have previously been proposed to serve as structural scaffolds in large multiprotein complexes (Hofmann and Bucher, 1998). The scPrp8p$^{2147–2397}$ structure presented here adds new facets to this hypothesis. Many primordial Jab1/MPN domain proteins do not exhibit long insertions or appendices but contain a JAMM motif (Tran et al., 2003) and therefore presumably act as metalloenzymes. Thus, our results suggest that the Prp8 Jab1/MPN-like domain represents a pseudoenzyme that has been converted into an adaptor protein in the course of its evolution. According to this line of thinking, Ub binding by the Prp8 element is a relic of an enzyme's affinity to its substrate. Another enzymatic vestige, the hydrophobic substrate binding channel, was apparently exploited to tightly attach a sequence insertion, the β5-β6 hairpin, to the Jab1/MPN core. Other portions of the surface, liberated from the constraints to support enzymatic activity, could likewise be used to firmly affix additional sequence elements (insertions and terminal appendices). The result is a mosaic, but nonetheless monolithic structure, in which five component parts (a Jab1/MPN-like core, an N-terminal appendix, two insertions, and a C-terminal appendix) are tightly interwoven (Figure 1D). The novel structural acquisitions now serve novel adaptor purposes. We suggest that Prp8 represents a functional paradigm for eukaryotic proteins with expanded Jab1/MPN domains (see also Supplemental Results and Discussion). In agreement with this notion, the C-terminal appendices of other family members have also been implicated in protein-protein interactions. For example, in the proteasome lid, the interaction of Rpn11 with another Jab1/MPN protein, Rpn8, requires the C-terminal flanking regions of both Jab1/MPN domains (Fu et al., 2001).

EXPERIMENTAL PROCEDURES

Protein Production

Proteins were expressed by established procedures in *Escherichia coli* using T7 promoter-based vectors. Soluble, recombinant proteins were captured on Ni-NTA resin (Qiagen), washed, and eluted with imidazole. The His_6 tags were cleaved with TEV protease, the samples were passed again over Ni-NTA, and the flowthrough fractions were further purified via Superdex 75 (Amersham Biosciences) gel filtration. Pure samples were concentrated to 25 mg/ml for crystallization. Further details for these and other methods are given in the Supplemental Data.

Crystallographic Analysis

scPrp8p$^{2147–2397}$ was crystallized in the presence of $BaCl_2$ with 2.5% PEG3350, 10 mM $CaCl_2$ as a reservoir. Crystals were cryoprotected with MPD and measured at 100 K on beamline BW6 (DESY, Hamburg, Germany). For structure solution, data from a SeMet-crystal were collected at three wavelengths around the Se K-edge. The structure was solved with SHELXD/E (http://shelx.uni-ac.gwdg.de/SHELX/index.html). Model building and refinement were conducted according to established procedures (Table 1).

Y2H Analysis

Y2H analyses were conducted as described previously (Liu et al., 2006).

Supplemental Data

Supplemental Data include Supplemental Results and Discussion, Supplemental Experimental Procedures, Supplemental References, and four figures and can be found with this article online at http://www.molecule.org/cgi/content/full/25/4/615/DC1/.

ACKNOWLEDGMENTS

This work was supported by the Max-Planck-Gesellschaft (to R.L. and M.C.W.), the Volkswagen Stiftung (to R.L. and M.C.W.), the Fonds der

Chemischen Industrie (to R.L.), and the Ernst-Jung-Stiftung (to R.L.). We thank Gleb Bourenkov (EMBL, Hamburg), Hannes Blume, Galina Kachalova, and Hans Bartunik (beamline BW6) for beamline support, Henning Urlaub for mass spectrometric analyses, Andreas Kuhn and Cindy Will for fruitful discussions and critically reading the manuscript. Author contributions: R.L. and M.C.W. conceived the project; V.P. did the cloning, expression, purification, and domain mapping of scPrp8p constructs; S.L. did the Y2H analyses and the associated cloning and mutagenesis; J.M.B. performed bioinformatics analyses; V.P. and M.C.W. carried out the crystallographic analyses; and all authors participated in data interpretation and writing of the paper.

Received: December 6, 2006
Revised: January 5, 2007
Accepted: January 18, 2007
Published: February 22, 2007

REFERENCES

Achsel, T., Ahrens, K., Brahms, H., Teigelkamp, S., and Lührmann, R. (1998). The human U5-220kD protein (hPrp8) forms a stable RNA-free complex with several U5-specific proteins, including an RNA unwindase, a homologue of ribosomal elongation factor EF-2, and a novel WD-40 protein. Mol. Cell. Biol. *18*, 6756–6766.

Ambroggio, X.I., Rees, D.C., and Deshaies, R.J. (2004). JAMM: a metalloprotease-like zinc site in the proteasome and signalosome. PLoS Biol. *2*, E2. 10.1371/journal.pbio.0020002.

Bellare, P., Kutach, A.K., Rines, A.K., Guthrie, C., and Sontheimer, E.J. (2006). Ubiquitin binding by a variant Jab1/MPN domain in the essential pre-mRNA splicing factor Prp8p. RNA *12*, 292–302.

Boon, K.L., Norman, C.M., Grainger, R.J., Newman, A.J., and Beggs, J.D. (2006). Prp8p dissection reveals domain structure and protein interaction sites. RNA *12*, 198–205.

Brenner, T.J., and Guthrie, C. (2005). Genetic analysis reveals a role for the C terminus of the Saccharomyces cerevisiae GTPase Snu114 during spliceosome activation. Genetics *170*, 1063–1080.

Cope, G.A., Suh, G.S., Aravind, L., Schwarz, S.E., Zipursky, S.L., Koonin, E.V., and Deshaies, R.J. (2002). Role of predicted metalloprotease motif of Jab1/Csn5 in cleavage of Nedd8 from Cul1. Science *298*, 608–611.

Fu, H., Reis, N., Lee, Y., Glickman, M.H., and Vierstra, R.D. (2001). Subunit interaction maps for the regulatory particle of the 26S proteasome and the COP9 signalosome. EMBO J. *20*, 7096–7107.

Grainger, R.J., and Beggs, J.D. (2005). Prp8 protein: at the heart of the spliceosome. RNA *11*, 533–557.

Hofmann, K., and Bucher, P. (1998). The PCI domain: a common theme in three multiprotein complexes. Trends Biochem. Sci. *23*, 204–205.

Kim, D.H., and Rossi, J.J. (1999). The first ATPase domain of the yeast 246-kDa protein is required for in vivo unwinding of the U4/U6 duplex. RNA *5*, 959–971.

Kuhn, A.N., Reichl, E.M., and Brow, D.A. (2002). Distinct domains of splicing factor Prp8 mediate different aspects of spliceosome activation. Proc. Natl. Acad. Sci. USA *99*, 9145–9149.

Laggerbauer, B., Achsel, T., and Lührmann, R. (1998). The human U5-200kD DEXH-box protein unwinds U4/U6 RNA duplices in vitro. Proc. Natl. Acad. Sci. USA *95*, 4188–4192.

Liu, S., Rauhut, R., Vornlocher, H.P., and Lührmann, R. (2006). The network of protein-protein interactions within the human U4/U6.U5 tri-snRNP. RNA *12*, 1418–1430.

Maytal-Kivity, V., Reis, N., Hofmann, K., and Glickman, M.H. (2002). MPN+, a putative catalytic motif found in a subset of MPN domain proteins from eukaryotes and prokaryotes, is critical for Rpn11 function. BMC Biochem. *3*, 28.

Raghunathan, P.L., and Guthrie, C. (1998). RNA unwinding in U4/U6 snRNPs requires ATP hydrolysis and the DEIH-box splicing factor Brr2. Curr. Biol. *8*, 847–855.

Reyes, J.L., Gustafson, E.H., Luo, H.R., Moore, M.J., and Konarska, M.M. (1999). The C-terminal region of hPrp8 interacts with the conserved GU dinucleotide at the 5′ splice site. RNA *5*, 167–179.

Schmidt, H., Richert, K., Drakas, R.A., and Kaufer, N.F. (1999). spp42, identified as a classical suppressor of prp4-73, which encodes a kinase involved in pre-mRNA splicing in fission yeast, is a homologue of the splicing factor Prp8p. Genetics *153*, 1183–1191.

Sloper-Mould, K.E., Jemc, J.C., Pickart, C.M., and Hicke, L. (2001). Distinct functional surface regions on ubiquitin. J. Biol. Chem. *276*, 30483–30489.

Small, E.C., Leggett, S.R., Winans, A.A., and Staley, J.P. (2006). The EF-G-like GTPase Snu114p regulates spliceosome dynamics mediated by Brr2p, a DExD/H box ATPase. Mol. Cell *23*, 389–399.

Staley, J.P., and Guthrie, C. (1998). Mechanical devices of the spliceosome: motors, clocks, springs, and things. Cell *92*, 315–326.

Than, M.E., Hof, P., Huber, R., Bourenkov, G.P., Bartunik, H.D., Buse, G., and Soulimane, T. (1997). Thermus thermophilus cytochrome-c552: A new highly thermostable cytochrome-c structure obtained by MAD phasing. J. Mol. Biol. *271*, 629–644.

Tran, H.J., Allen, M.D., Lowe, J., and Bycroft, M. (2003). Structure of the Jab1/MPN domain and its implications for proteasome function. Biochemistry *42*, 11460–11465.

Turner, I.A., Norman, C.M., Churcher, M.J., and Newman, A.J. (2006). Dissection of Prp8 protein defines multiple interactions with crucial RNA sequences in the catalytic core of the spliceosome. RNA *12*, 375–386.

Valadkhan, S., and Manley, J.L. (2001). Splicing-related catalysis by protein-free snRNAs. Nature *413*, 701–707.

van Nues, R.W., and Beggs, J.D. (2001). Functional contacts with a range of splicing proteins suggest a central role for Brr2p in the dynamic control of the order of events in spliceosomes of Saccharomyces cerevisiae. Genetics *157*, 1451–1467.

Verma, R., Aravind, L., Oania, R., McDonald, W.H., Yates, J.R., 3rd, Koonin, E.V., and Deshaies, R.J. (2002). Role of Rpn11 metalloprotease in deubiquitination and degradation by the 26S proteasome. Science *298*, 611–615.

Will, C.L., and Lührmann, R. (2006). Spliceosome structure and function. In The RNA World, T. Cech and J. Atkins, eds. (Cold Spring Harbor, NY: Cold Spring Harbor Laboratory Press), pp. 369–400.

Yao, T., and Cohen, R.E. (2002). A cryptic protease couples deubiquitination and degradation by the proteasome. Nature *419*, 403–407.

Accession Numbers

Coordinates and structure factors have been submitted to the Protein Data Bank (http://www.rcsb.org/pdb/) under accession code 2OG4.